

Optimal sequential sampling design for environmental extremes

Raphaël de Fondeville and Matthieu Wilhelm

February 4, 2022

Abstract

The Sihl river, located near the city of Zurich in Switzerland, is under continuous and tight surveillance as it flows directly under the city’s main railway station. To issue early warnings and conduct accurate risk quantification, a dense network of monitoring stations is necessary inside the river basin. However, as of 2021 only three automatic stations are operated in this region, naturally raising the question: how to extend this network for optimal monitoring of extreme rainfall events?

So far, existing methodologies for station network design have mostly focused on maximizing interpolation accuracy or minimizing the uncertainty of some model’s parameters estimates. In this work, we propose new principles inspired from extreme value theory for optimal monitoring of extreme events. For stationary processes, we study the theoretical properties of the induced sampling design that yields non-trivial point patterns resulting from a compromise between a boundary effect and the maximization of inter-location distances. For general applications, we propose a theoretically justified functional peak-over-threshold model and provide an algorithm for sequential station selection. We then issue recommendations for possible extensions of the Sihl river monitoring network, by efficiently leveraging both station and radar measurements available in this region.

1 Introduction

During summer 2005, the city of Zurich was heavily flooded causing six deaths and inducing an estimated property damage of around 3 billions Swiss francs (Bezzola and Hegg, 2007). As illustrated by Figure 1, the lake side location of Zurich makes the city particularly prone to flood risk, especially that several rivers flow directly through its center. One of these rivers, the Sihl, is particularly monitored as its waterbed is located directly under the city main railway station, which is partly built underground. Thus Sihl extreme water heights are likely to cause hundreds of millions of francs of losses by damaging existing infrastructures and by preventing half a million commuters from travelling.

Following the 2005 flood, which fortunately spared the Sihl, an overall assessment of flood risk for the city has been conducted, leading to a new local policy for disaster risk reduction. As a consequence, civil engineering infrastructures to minimize long term risk exposure were constructed. These were combined to short term mitigation measures, namely a system of “early warnings”, which relies on weather forecasts and delivers to populations and authorities messages of likely flooding in the coming hours. In both cases, these protective measures require to monitor rainfall extremes as accurately as possible, to adequately calibrate the infrastructure in the first case, and minimize false alarms in the second.

To this end, the main sources of rainfall measurements are weather stations, represented by crosses in Figure 1. Of all sources, this kind of observations have usually the longest temporal coverage: for instance in Switzerland, oldest rainfall records dates from 1863. These measures are however sparse in space, only 14 around the Sihl river with only 3 of them located inside

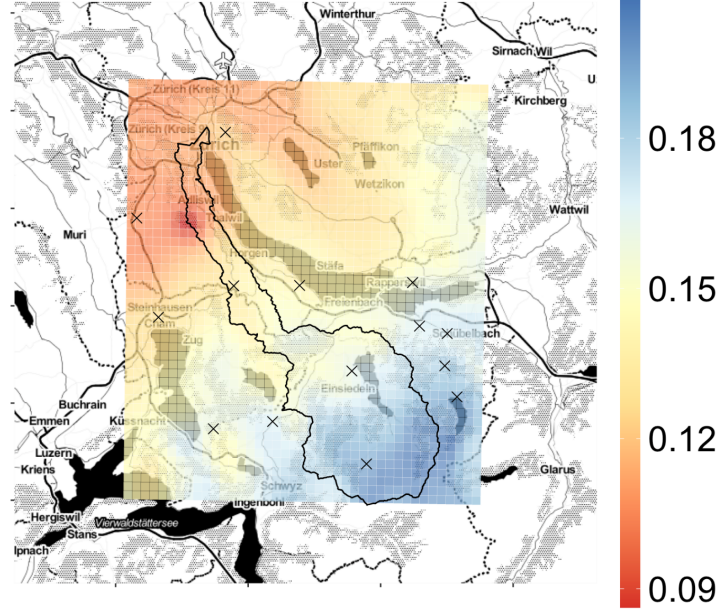


Figure 1: Hourly mean rainfall (mm) from radar measurements over the period 2013 to 2018 around the Sihl river basin. The solid black line delimits the Sihl river basin while black crosses represent the locations of the 14 weather stations installed by MeteoSwiss.

the basin, and may suffer from multiples sources of uncertainties such as weather conditions, e.g., wind or snow, right censoring or instruments changes. As the only source of direct measurements, station data is in general considered as most accurate for risk quantification.

With the raise of new technologies, radar measurements are now much more frequently available: for instance “CombiPrecip” produced by MeteoSwiss (Sideris et al., 2014; Gabella et al., 2017; Panziera et al., 2018) provides spatially dense estimates of temporally accumulated rainfall at high spatial resolution since 2013. These observations are however indirect and result from processing radio waves acquisitions, which are usually subject to strong bias and distortion, especially in region with altitude variation. There is usually a large discrepancy between measurements provided by radar products and by weather stations, and their relationship is today far from being understood. For this reason, radar products are, as of today, almost exclusively used for short term mitigation and need to be combined to station measurements to correct potential biases in intensity.

Techniques for flood risk quantification, both long and short term, relies on catalogues of heavy rainfall events that are then fed to a hydrological numerical model which translates the event into water runoffs. These catalogues are either historical, i.e., derived from available measurements, or produced by weather generators that can be either numerical (Cloke and Pappenberger, 2009) or stochastic (see, e.g., Furrer and Katz, 2008; de Fondeville and Davison, 2021); in the latter extreme value theory offers a mathematically justified framework to model and extrapolate extreme water levels. In both cases, the methodologies extrapolate stations measurements away from monitoring sites to estimate the water distribution over the region of interest. The accuracy of such techniques is thus tightly linked to the number of monitoring stations present in the basin. For the Sihl river, as of 2021, only three stations provides automatic rainfall measurements, and because of the importance of the infrastructure at risk, it would be

necessary to extend the network of station for optimal monitoring of extreme rain events.

In this work, we define and explore sampling designs for optimal monitoring of extremes events, with the goal to efficiently extend the existing network of stations in the Sihl river basin. More precisely, we propose a model based on extreme value theory that leverages the strength of both station and radar measurements and issue recommendations for candidate locations of new stations. Section 2 reviews classical principles for sampling design over compact spaces, proposes a new paradigm for extreme monitoring and derives its properties for stationary random fields. Section 3 presents functional peaks-over-threshold analysis by describing the asymptotic tail behaviour of stochastic processes, that is then combined with the previously introduced principle for sampling design to provide explicit model and algorithm to optimal monitoring of extremes. Section 4 details the Sihl case study and provides recommendation to extend the current network of measurement stations. Finally, Section 5 concludes with the limitations of the current model and possible improvements for future research.

2 Monitoring extremes of random fields on compact sets

2.1 Related literature

Stations networks are installed to fulfil one or several, possibly contradicting, monitoring purposes (Chang et al., 2007): their design can be thus formulated as an optimization problem, potentially under constraints such as budget or landscapes regulations, with a clear objective function to be minimized (p. 502, Zidek and Zimmerman, 2019). Depending on choice of objective, data availability, and, field assumptions, network designs are classified as geometry, probability and model based. All three categories rely on the minimal assumption that the process X to be monitored is continuous over the region S of interest, that we assume bounded.

The first approach, also known as space-filling designs, exploits only the geometrical properties of S , and as such, is useful when little to no information is available about the monitoring purpose object; see, e.g., Pronzato and Müller (2012) for an extensive review of such designs. Networks derived from this principle turned out to be performing well in settings where dependence is known and the network purpose is limited to spatial prediction (Li and Zimmerman, 2015); they can perform quite poorly in other contexts.

Probability based designs, also known simply as ‘design-based’ in survey sampling, consider the object of monitoring to be deterministic, but makes stations locations random by imposing a model on their distribution; see Tillé and Wilhelm (2017) for a recent review of such techniques. One of their appealing property is the intrinsic agnostic nature of the design: stations are selected with the help of a prescribed distribution and no modelling assumption is made on the field X . For this reason, probability based designs are often considered as ‘free’ from any kind of subjective bias induced by any prior knowledge on X or the geometry of S . These techniques have been mostly developed for optimal estimation of the mean or the cumulative distribution function of the process. While they can be used outside this scope, their performance is usually not ensured.

The third, and last, class of designs assumes that X is a continuous stochastic process over S whose distribution is given by a model imposed by the designer and tailored to reflect the specificities of the network purpose(s). In this case, the set of stations induced by the sampling design is skewed by the incorporation of prior knowledge, making its performance determined by the model’s validity. In this context, an attractive objective function is one that selects locations such that model’s parameters estimates, e.g., covariance functions parameters (Müller and Zimmerman, 1999), have minimal uncertainty. However, in general, there is a trade-off between optimal parameters estimation and minimal prediction error at unmeasured

locations. [Zidek and Zimmerman \(2019\)](#) argues that entropy, which aims at optimally reducing the uncertainty of predictions at unmeasured locations, achieves a compromise between both previous objectives.

In absence of collected data, a setting that is known as “optimal design of experiments” in statistics, model estimation is likely to not be possible, and we need to make potentially strong hypotheses on the distribution of X , the most common being strict stationarity. [Pukelsheim \(2006\)](#) provides an exhaustive review of this branch of statistics, that [Zidek and Zimmerman \(2019\)](#) refers to as *de novo* design. Alternatively, when data is available, a more general model, whose flexibility depends on the quantity and quality of available data, can be fitted to compute optimal sets of measurement stations.

Model based designs leveraging existing data are tightly linked to the literature on design of computer experiment ([Santner et al., 2018](#)), which mostly relies on Gaussian processes. Theoretical properties of Gaussian designs have been studied for multiple purposes such as global optimization ([Jones et al., 1998](#)), environmental risk assessment ([Arnaud et al., 2010](#); [Chevalier et al., 2014](#); [Azzimonti et al., 2016, 2019a](#)) and uncertainty quantification for level sets ([Azzimonti et al., 2019b](#)). In particular, [Bect et al. \(2012\)](#) propose network designs to detect probabilities of failure, i.e., finding regions, called excursion sets, where the probability of the Gaussian process X to exceeds a threshold u is greater than some quantile of reference ([Adler and Taylor, 2007](#)); subsequent research in the same area includes [Chevalier et al. \(2014\)](#) and [Azzimonti et al. \(2016, 2019a\)](#). While Gaussian processes are attractive for versatility and convenience, assuming normal distributions is likely to strongly under-estimate rare extreme events with potentially dire consequences for purposes such as risk quantification of potentially heavy-tailed processes.

The literature on network design for monitoring of extreme events is, to this date, rather limited: [Chang et al. \(2007\)](#) discuss the challenges arising in the design of networks for extremes monitoring. For this specific purpose, they give evidences against classical designs and propose a Bayesian hierarchical model with a Gaussian copula with good empirical performance, but do not “appeal to an axiomatic theory as in the classical theory of extremes”, which is the goal of the current work. More recently, [Hainy et al. \(2016\)](#) propose a model for optimal monitoring of yearly maxima using extreme value theory that they use to rank existing stations within a network as function of their impact on the estimation accuracy. In this work, we propose to monitor single extreme events, defined as specific types of exceedances, instead of maxima and propose a principled approach to the general problem of sampling designs for optimal monitoring of extremes.

2.2 Principle of sampling designs for extremes

When studying extremes, the definition of an objective function for the optimization of the sampling process must be carefully considered. Indeed, variance reduction under an unbiasedness constraint, which is classically used for sampling design, is not a good criterion: first it sets the focus on the accurate estimation of the process mean, and second, variance might even not exist if the process is sufficiently heavy-tailed. For this reason, we propose an alternative criterion for extremal sampling design based on a risk measure.

For univariate quantities, risk can be characterized by the distribution of exceedances over a high threshold, whose value can be chosen, for instance, as the minimum over which damages occur. For random fields, the notion of exceedance, and so of risk, is however not unique. In this case, we rely on the notion of r -exceedance ([Dombry and Ribatet, 2015](#)) for which a stochastic process X over a compact domain S is summarized by a univariate summary statistics $r(X)$ computed with the help of a risk functional r . In this case, an extreme event is defined as an

exceedance of the functional $r(X)$ over the threshold u . The functional r characterizes the risk under study, for instance, in case of rainfall, it may distinguish different underlying physical processes, e.g., cyclonic or convective rain. Indeed, both types of rainfall event are driven by different physical laws, producing rain fields with different spatio-temporal structures. The role of risk functional in this case is thus to disentangle both type of extreme events, see [de Fondeville and Davison \(2021\)](#) for a detailed illustration.

Popular choices of risk functionals are for instance $r(X) = \sup_{s \in S} X(s)$, where events with at least one location above a threshold are considered as extremes or $r(X) = \int_0^T \int_S X(s, t) ds dt$, which computes, when X represents the rain field, the volume of water fallen over the region S over the time window $[0, T]$. In any case, it defines a measure of the severity of the event.

Suppose now that we can evaluate the process X only at a limited number of sites $L > 0$, determined for instance by the available budget to install measuring equipment. We wish to find an optimal set of L locations, say $S_{\text{samp}} \subset S$ such that the risk is best quantified, i.e., such that

$$S_{\text{samp}} = \underset{\{s_1, \dots, s_L\} \subset S}{\operatorname{argmin}} \left| \Pr \{r(X) \geq u\} - \Pr \{r_{\{s_1, \dots, s_L\}}(X) \geq u | r(X) \geq u\} \right|, \quad (1)$$

where $r_{\{s_1, \dots, s_L\}}(X)$ is a consistent estimator of $r(X)$, i.e., a quantity derived from the vector $\{X(s_1), \dots, X(s_L)\}$ and such that $r_{\{s_1, \dots, s_L\}}(X) \rightarrow r(X)$ as $L \rightarrow \infty$, in some sense. Simple examples of discretization of $r(X) = \sup_{s \in S} X(s)$ and $r(X) = \int_S X(s) ds$ are $\max_{s \in S_{\text{samp}}} X(s)$ and $L^{-1} \sum_{i \in S_{\text{samp}}} X(s_i)$ respectively, and the convergence (in probability) occurs for instance if $S_{\text{samp}} \stackrel{\text{i.i.d}}{\sim} \mathcal{U}(S)$, where \mathcal{U} denotes the uniform distribution on S . Thus, sampling design minimizing (1) will provide a set of locations for which the probability of the risk $r(X)$ to exceeds threshold $u \in \mathbb{R}$ is best approximated using the process sampled at locations in S_{samp} .

A sample S_{samp} as defined by (1) is meaningful for both long and short term risk mitigation: the construction of civil engineering infrastructure necessitates an adequate quantification of the risk and early warnings are usually defined by hazards levels, which are derived from probability of exceeding certain levels of intensity. In the latter case, false negative are likely to have dire consequences, as population might not be informed of an imminent natural disaster, and thus it is critical that the network of station minimizes (1) as much as possible. For risk estimation, the analysis relies in general on a model estimated using all observation for which there is a significant risk, i.e., using the previous definition, such that $r(X) > u$. Thus accurate risk estimation is tightly linked by our capability to accurately estimate $\Pr\{r(X) \geq u\}$ from its discretization.

Finally, we could also have considered alternative criteria such as minimizing the absolute difference between $\mathbb{E}\{r(X)\}$ and the expectation of its estimator for finite L . This choices would however be less general as it requires to suppose the existence and finiteness of such quantities, which is non-trivial to prove for most of existing random fields.

2.3 Properties of sampling designs for extremes of stationary processes

We now study the properties of the sampling design over a compact domain $S \subset \mathbb{R}^d$ induced by the equation (1) for stationary processes X . Although rarely satisfied in practice, stationarity is a convenient working hypothesis when little to no a priori information about the tail distribution of the data is available or when trying to understand the theoretical properties of stochastic processes. We thus suppose that X is strictly stationary, i.e., for any locations $s_1, \dots, s_L \in S$, direction h in the $d - 1$ unit sphere \mathbb{S}^{d-1} , and scalar $t > 0$, we assume that

$$\Pr\{X(s_1) \leq x_1, \dots, X(s_L) \leq x_L\} = \Pr\{X(s_1 + th) \leq x_1, \dots, X(s_L + th) \leq x_L\}, \quad x \in \mathbb{R}^L.$$

From the point of view of extremes, stationarity implies that for any threshold $(u_1, u_2) \in \mathbb{R}^2$,

$$\pi(S_1, S_2) = \Pr\{\sup_{s \in S_1} X(s) \geq u_1, \sup_{s \in S_2} X(s) \geq u_2\}, \quad S_1, S_2 \subset \mathbb{R}^d, \quad (2)$$

is invariant by translation of S_1 and S_2 . The function π can be used as a measure of spatial dependence and its limit for increasingly large threshold when divided by $\Pr\{\sup_{s \in S_1} X(s) \geq u\}$ is commonly used to quantify extremal dependence (Ledford and Tawn, 1996; Engelke et al., 2019).

To describe the properties of the sampling design induced by (1), we will assume that π is a decreasing function of the distance between S_1 and S_2 , i.e., the probability that the process X exceeds a potentially large threshold simultaneously on two regions, decreases as a function of the distance separating them. This hypothesis is natural for environmental applications and translates, for the analysis of extremes, the First Law of Geography (Tobler, 1970), i.e., ‘everything is related to everything else, but near things are more related than distant things’. In classical spatial statistics, an equivalent hypothesis would simply assume that the covariance function is decreasing with the distance.

To avoid any contradiction with Tobler’s law, the probabilistic nature of π requires further assumptions to discard the possibility to find conditions for which there exists a vector $h_1 \in \mathbb{S}^{d-1}$ and $t > 1$ such that $\pi(S_1, S_2 + th_1) > \pi(S_1, S_2 + h_1)$. To do so, we introduce the notion of hitting scenario: for a threshold u , we call a hitting scenario a function H which for any pair $(S_1, S_2) \subset S \times S$ associates a partition $H(S_1, S_2) = \{H_k\}_{k=1}^K$ of the set $\{x \in C(\mathbb{R}^d) : \sup_{s \in S_1} X(s) \geq u, \sup_{s \in S_2} X(s) \geq u\}$. For instance, a simple hitting scenario distinguishes between random paths over S for which $\sup_{s \in S_1} X(s) > \sup_{s \in S_2} X(s)$. In other words, these scenarios allow to characterize more precisely the context in which joint exceedances take place, similarly to the work of Wang and Stoev (2013) for maxima: both notions share the underlying idea to distinguish between the different paths yielding to a same observed event.

Assumption 1. For any convex $S \subset \mathbb{R}^d$, vector $h \in \mathbb{S}^{d-1}$ and hitting scenario H ,

$$\pi_H(S, S + th) = \Pr\{\sup_{s \in S} X(s) \geq u, \sup_{s \in S+th} X(s) \geq u, X \in H_k\}, \quad k = 1, \dots, K$$

is a decreasing function of $t > 0$.

Intuitively, Assumption 1 formally translates the first law of geography for the dependence measure (2). Omitting hitting scenarios would not ensure that, when analyzing the different paths yielding joint exceedances, it is not possible to find a configuration under which there exists $t > 1$ and $h \in \mathbb{S}^{d-1}$ such that $\pi_H(S, S + th) > \pi_H(S, S + h)$, for which Tobler’s law is obviously violated.

Example. Let X be a continuous stationary Gaussian process with decreasing covariance function σ and mean 0. Consider $S_1 = \{s_1\} \subset S$ and $S_2 = \{s_2\} \subset S$ and the hitting scenario

$$H : (s_1, s_2) \rightarrow \{x \in C(S) : (-1)^i \times \{x(s_1) > x(s_2)\}\}_{i=1,2},$$

then

$$\pi_H[\{s_1\}, \{s_2\}] = \Phi_{0, \Sigma}(-u, -u)/2,$$

where $\Phi_{0, \Sigma}$ is the distribution function of a bivariate normal random variable with zero mean and covariance $\Sigma = \{\sigma(s_i - s_j)\}_{i,j=1,2}$, and thus π_H is a decreasing function of the distance between S_1 and S_2 . A similar formula can be derived for generalized r -Pareto process; see Section 3.1.

In some cases, the risk functional and its discretization can be ordered: for instance, the supremum over S is always greater than its discretization, and (1) simplifies to

$$S_{\text{samp}} = \operatorname{argmax}_{\{s_1, \dots, s_L\}} \Pr \left\{ \max_{s \in \{s_1, \dots, s_L\}} X(s) \geq u \mid \sup_{s \in S} X(s) \geq u \right\}. \quad (3)$$

Similar simplifications, with possibly reverse relations, also holds for the infimum. For the analysis of extremes, the supremum functional is a common choice that we choose to focus on: for locations $s_1, \dots, s_L \in S$, we observe that

$$\begin{aligned} & \Pr \left\{ \max_{s \in \{s_1, \dots, s_L\}} X(s) \geq u \mid \sup_{s \in S} X(s) \geq u \right\} \\ &= \sum_{i=0}^{L-1} \Pr \left\{ X(s_{i+1}) \geq u \mid \sup_{s \in S} X(s) \geq u \right\} - \sum_{i=1}^{L-1} \Pr \left\{ X(s_{i+1}) \geq u, \max_{s \in \{s_1, \dots, s_i\}} X(s) \geq u \mid \sup_{s \in S} X(s) \geq u \right\} \end{aligned} \quad (4)$$

$$= \Pr \left\{ X(s_1) \geq u \mid \sup_{s \in S} X(s) \geq u \right\} + \sum_{i=1}^{L-1} \Pr \left\{ X(s_{i+1}) \geq u, \max_{s \in \{s_1, \dots, s_i\}} X(s) \leq u \mid \sup_{s \in S} X(s) \geq u \right\}, \quad (5)$$

allowing to elucidate the nature of optimal sampling designs induced by criteria (3). Because of stationarity, marginal probabilities in (4) do not influence the design choice, so, at first sight, solving (3) under Assumption 1 seems equivalent to maximize inter-points distances, i.e., an optimal sampling design would, roughly speaking, cover S as extensively as possible. However, condition $\sup_{s \in S} X(s) \geq u$ induces a boundary effect, whose strength is function of the dependence, making terms in (5) to be influenced not only by the distances between sampling locations but also by their position with respect to the boundary ∂S of S .

Theorem 1. *Let X be a stationary stochastic process with sample path on $C(\mathbb{R}^d)$ satisfying Assumption 1 and S a compact set in \mathbb{R}^d . For any convex subset $S_1 \subset S$, the probability*

$$\Pr \left\{ \sup_{s \in S_1} X(s) \geq u, \sup_{s \in S \setminus S_1} X(s) \leq u \right\}, \quad u \in \mathbb{R},$$

is a decreasing function of $\operatorname{dist}(S_1, \partial S) = \inf_{s \in S_1, s' \in \partial S} \|s - s'\|$, where ∂S represents the boundary of S .

Theorem 1, whose proof can be found in Appendix B, reveals that the supremum of stochastic processes is more likely to be located close to the boundary ∂S of S . Such boundary effect influences solutions to (3) and, depending of the strength of dependence, favours points on, or close to ∂S . Figure 2 illustrates this phenomenon for two classical models of stochastic processes and different level of dependence; see Appendix A for simulation details. We observe that exceedances above the threshold $u = 1$ are more likely on and close to the boundaries. We also note that the boundary effect vanishes as soon as the set S_h reaches a distance greater than the dependence range: this phenomenon is observed for the second type a Gaussian process with weak dependence and, more generally, for any process for which (near)-independence is achieved for large distances. Examining equation (5) in light of Theorem 1 shows a salient aspect of the optimization of sampling designs for monitoring extremes: it yields non-trivial points patterns that results from a compromise between a boundary effect and maximization of inter-location distances.

One way to mitigate the boundary effect is to search for candidate locations not exclusively within S but in a region including S and its extension up to the effective range of dependence

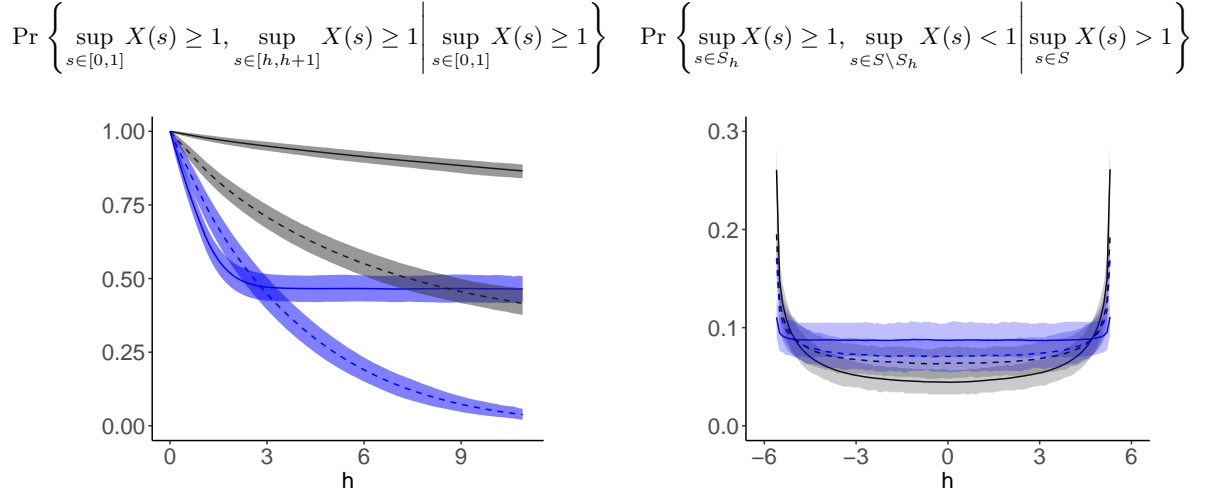


Figure 2: Left: Estimated probabilities of concurrent exceedances as a function of the distance h for four stationary processes. Right: Estimated probabilities that the process X exceeds 1 on the interval $S_h = [h - 0.5, h + 0.5]$ only as a function of its location $h \in [-5.5, 5.5]$ in $S = [-6, 6]$ when X satisfies $\sup_{s \in S} X(s) \geq 1$ (right). Estimates are obtained by simulation of Gaussian processes (solid line) and generalize r -Pareto process (dashed lines), for strong dependence (black) and weak dependence (blue).

in all directions. In this case, points inside S are, not surprisingly, systematically favoured as $\Pr \{X(s_1) \geq u | \sup_{s \in S} X(s) \geq u\}$ in (4) is maximal, and constant, for any $s_1 \in S$. In this case, the boundary effect is smoothed but the induced monitoring network is meant to be exposed to false positives. In the absence of boundaries, e.g., if S is a compact manifold, the sampling scheme simply cover the space as well as possible by maximizing the inter-locations distances corresponding to space-filling points sets, as a consequence of Assumption 1.

We should stress once again that all the previous developments rely on Assumption 1 and simplification (3), and do not require hypotheses on the asymptotic tail behaviour of the process, as it is commonly done in extreme value theory. Thus, any process whose dependence for finite threshold u decreases with the distance exhibit such boundary effect. These results however rely on strict stationarity, which is unrealistic for most applications. When some a priori information is available, for instance from existing measurement stations, or from other indirect measurements, generalized r -Pareto processes can be leveraged to find near-optimal sampling designs without assuming strict stationarity.

2.4 Algorithm for optimal sequential sampling design

Solving (1) in its general form is intractable, so in practice we resort to a discretization of the region of interest. The resolution of the grid is determined by the desired spatial precision of the solution and the accuracy of the probabilities estimates. Even with such setting, tractability of the optimization cannot be ensured when searching for sets of size larger than 3 because of the combinatorial nature of the problem. We therefore suggest a sub-optimal, but tractable, method to solve (1), i.e., we propose to search optimal sequential designs using Algorithm 1. This procedure is general, applicable to any risk functional, and for the special case of the

Algorithm 1: Sequential algorithm for extremal sampling design.

```

Input number of location  $L$ ;
Optional: initial set of points  $S_{\text{samp}}$  ;
if  $S_{\text{samp}} = \emptyset$  then
    Choose initial point preferably either at random or using geometrical information
    on  $S$ ;
end
for  $i$  from  $L_{\text{samp}} + 1$  to  $L$  do
    Solve  $s_{\text{add}} = \arg \min_{s \in S} |\Pr \{r(X) \geq u\} - \Pr \{r_{\{s_1, \dots, s_{i-1}, s\}}(X) \geq u | r(X) \geq u\}|$ ;
    Set  $S_{\text{samp}} = S_{\text{samp}} \cup \{s_{\text{add}}\}$ 
end
return  $S_{\text{samp}}$ .

```

supremum, provides an optimal set of locations as

$$\begin{aligned}
& \Pr \left\{ \max_{s \in \{s_1, \dots, s_L\}} X(s) \geq u \mid \sup_{s \in S} X(s) \geq u \right\} \\
&= \Pr \left\{ \max_{s \in \{s_1, \dots, s_{L-1}\}} X(s) \geq u \mid \sup_{s \in S} X(s) \geq u \right\} \\
&+ \Pr(X(s_L) \geq u \mid \sup_{s \in S} X(s) \geq u) - \Pr \left(X(s_L) \geq u, \max_{s \in \{s_1, \dots, s_{L-1}\}} X(s) \geq u \mid \sup_{s \in S} X(s) \geq u \right). \quad (6)
\end{aligned}$$

Indeed, the first term of the right hand side of (6) is fixed given s_1, \dots, s_{L-1} , while the others depend only on s_L . Thus, sequentially maximizing the left hand side of (6) is equivalent to optimize the last two terms of the right side, and thus explicitly follows the principles derived from Theorem 1.

Figure 3 illustrates the procedure described in Algorithm 1; in this experiment, probabilities are estimated empirically using 10^6 simulations of a weakly dependent r -generalized Pareto process as in Figure 2 and rescaled to 0 and 1 for easier visualization. We consider two initialisation: first, two stations located on the boundary of $[-6, 6]$ as prescribed by Theorem 1 and, second, two stations selected at random. In the latter, we observe that, as a consequence of the phenomenon described by Theorem 1, locations on the boundaries are quickly sampled.

In case where the interest lies beyond sequential design, Algorithm 1 can be adapted to include a forward-backward steps such as in Zhang (2011). One could also consider k -look ahead strategies, that is the simultaneous inclusion of k measurement stations. In the application described in Section 4, the implementation of a forward-backward step does not change significantly the selected locations.

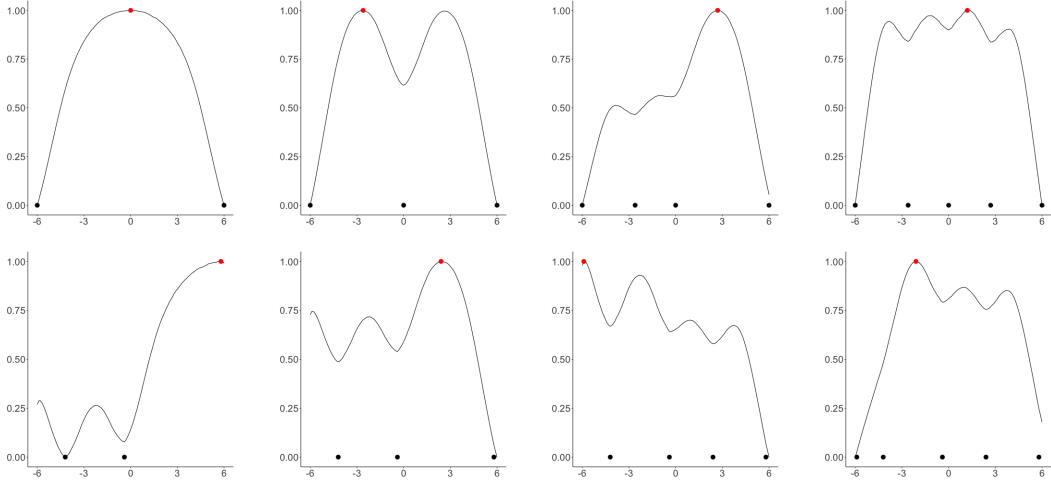


Figure 3: Illustration of Algorithm 1 for sequential addition of 4 locations with boundary (top) and random (bottom) initialization. The curves represent the (conditional) probability of exceedance and are estimated empirically from 10^6 simulation of an extremal stationary process satisfying $\sup_{s \in [-6,6]} x(s) \geq 1$ and scaled to varies between 0 and 1.

3 Extremal sampling designs using extreme value theory

3.1 Peaks-over-threshold analysis

Extreme value theory was first introduced for block maxima, describing the limit distribution of

$$M_n = \max_{i=1,\dots,n} X_i, \quad \text{as } n \rightarrow \infty,$$

where X_i are independent and identically distributed random variables (e.g., [Fisher and Tippett, 1928](#); [Gnedenko, 1943](#)). However, for more accurate risk quantification and optimal monitoring of extremes toward efficient early warnings of natural disasters, we need to study single events with potentially large values, i.e., tail distributions of stochastic processes. For this reason, we focus on an alternative view on extremes called peaks-over-threshold analysis ([Balkema and de Haan, 1974](#); [Pickands, 1975](#); [Davison, 1984](#)).

Let X be a random variable, then for any threshold $u < \inf\{x : F(x) = 1\}$, under some mild conditions we can find sequences $a_n > 0$ and b_n such that

$$\left. \begin{aligned} n \Pr \left\{ \left(1 + \xi \frac{X - b_n}{a_n} \right)_+^{1/\xi} \geq x \right\}, & \quad \xi \neq 0, \\ n \Pr \left\{ \exp \left(\frac{X - b_n}{a_n} \right)_+ \geq x \right\}, & \quad \xi = 0, \end{aligned} \right\} \rightarrow x^{-1}, \quad n \rightarrow \infty, \quad (7)$$

where $(\cdot)_+ = \max(\cdot, 0)$. In practice, (7) means that the conditional distribution of exceedances over a high threshold can be approximated by a generalized Pareto distribution. The parameter ξ , called the tail index, determines the strength of the tail and its support: for $\xi > 0$, $x \geq u$ and the tail decay is polynomial (Fréchet), for $\xi = 0$, $x \geq u$ and the tail has an exponential decay (Gumbel), and finally for $\xi < 0$, $x \in (u; u - \sigma/\xi)$ and we retrieve a polynomial tail decay (Weibull). This result has been generalized to a multivariate setting ([Rootzén and Tajvidi, 2006](#); [Rootzén et al., 2018a,b](#)), and more recently to functions ([de Fondeville and Davison, 2021](#)).

Again, let S be a compact subset of \mathbb{R}^d representing the region under consideration and $C(S)$ denotes the space of real-valued continuous functions over S . We now consider that X refers to

a stochastic process with sample path in $C(S)$. In a univariate context, it is straightforward to define the notion of exceedance, but for functions, it needs to be carefully introduced. Following [Dombry and Ribatet \(2015\)](#) and [de Fondeville and Davison \(2018\)](#), we consider a functional $r : C(S) \rightarrow \mathbb{R}$, called a risk functional, which computes a univariate summary of the stochastic process X and defined an r -exceedance as an event $\{r(X) \geq u\}$ where $u \geq 0$ is a threshold of choice.

We now suppose that there exist sequences of functions $a_n \in C(S, (0, \infty))$ and $b_n \in C(S)$ and a scalar $\xi \in \mathbb{R}$ such that

$$n \Pr \left\{ \left(1 + \xi \frac{X - b_n}{a_n} \right)^{1/\xi} \in \cdot \right\} \rightarrow \Lambda(\cdot), \quad (8)$$

where Λ is a non-degenerate measure on $\mathcal{F} = C(S, (0, \infty)) \setminus \{0\}$. Equation (8) is a natural extension of the univariate condition (7) for convergence of the tail distribution towards a generalized Pareto distribution and implies that

$$\Pr \left[\frac{X - b_n}{a_n} \in (\cdot) \middle| r \left\{ \frac{X - b_n}{a_n} \right\} \geq 0 \right] \rightarrow \Pr\{P \in (\cdot)\}, \quad n \rightarrow \infty, \quad (9)$$

where P is a generalized r -Pareto process; detailed conditions on the functional r can be found in [de Fondeville and Davison \(2021\)](#).

The generalized r -Pareto process P is parametrized by a tail index ξ function and a limit measure Λ , respectively characterizing the regime of marginal tail decay and extremal dependence. This class of processes is a natural extension of univariate peaks-over-threshold analysis to functions. In particular, for any $s \in S$ and sufficiently high threshold $u \geq 0$,

$$\Pr\{P(s) \geq u + x \mid P(s) \geq u\} = 1 - F_{\xi, \sigma(u)}(x),$$

where $\sigma(u) = 1 + \xi u$ and $1 - F_{\xi, \sigma(u)}$ is the survival function of a generalized Pareto random variable. However, we request that the measure Λ is non-zero on the space of continuous functions on S , which restricts the model to one particular case of extremal dependence, namely asymptotic dependence. This implies that the strength of the dependence decreases but stabilizes as the intensity of the event increases, i.e., there exists for each location in $s \in S$ a neighbourhood for which points are positively associated with $X(s)$ independently of the marginal intensity.

Generalized r -Pareto processes are constructed using the representation

$$P = \frac{\{RW/r(W)\}^\xi - 1}{\xi}, \quad (10)$$

where R is a univariate unit Pareto random variable and W is a stochastic process on the unit L_1 -sphere $\{x \in C(S) : \|x\|_1 = 1\}$ whose distribution is determined by Λ and models the dependence of P . Equation (10) is a key component to sampling algorithms as the ones described in [de Fondeville and Davison \(2021\)](#). In general, the process W can take any kind of distribution as soon as $\mathbb{E}\{W(s)\} = 1$ for all $s \in S$.

Assuming that the tail index ξ is homogeneous over S is common in environmental applications (e.g., [Ferreira et al., 2012](#); [Engelke et al., 2019](#)), especially when the region of interest is small relative to the scale of the process under study. In this case, the tail index ξ characterizes not local tail behaviors but the tail regime of the physical process itself, e.g., a specific type of rainfall. Visual diagnostics, such as qq-plots, allows to assess the reliability of such assumption. In general, the latter can be relaxed, but then, using an asymptotically justified model requires to define exceedances on the re-normalized process $Y = \{1 + \xi(X - b_n)/a_n\}^{1/\xi}$, with the risk to lose any potential physical interpretation.

To model extremal dependence, a very convenient model for W is a stationary log-Gaussian random field, for which extremal dependence is simply summarized by

$$\rho(h) = \Pr\{P(s+h) \geq u \mid P(s) \geq u\} = 2 \left(1 - \Phi \left[\left\{ \frac{\gamma(h)}{2} \right\}^{1/2} \right] \right), \quad (11)$$

where u is a sufficiently large threshold, γ is the semi-variogram of the underlying Gaussian process and Φ is the distribution function of a standard normal random variable. The function ρ is called the extremogram (Davis and Mikosch, 2009), or the χ coefficient in a multivariate setting (Ledford and Tawn, 1996), and measures pairwise extremal dependence. Indeed, for heavy-tailed processes, classical measures of dependence such as a covariance function does not necessarily exist, and thus we require alternatives such as the extremogram. This model is convenient as it allows to leverage existing Gaussian dependence models from the literature on spatio-temporal statistics to drive the extremal dependence of P .

In practice, following asymptotic convergence (9), the distribution of functional exceedances can be approximated by a generalized r -Pareto process, i.e.,

$$\Pr \left[\frac{X - b_n}{a_n} \in \cdot \mid r \left\{ \frac{X - b_n}{a_n} \right\} \geq 0 \right] \approx \Pr\{P \in \cdot\} \quad (12)$$

where the functions a_n and b_n are also unknown and need to be estimated. When the risk functional is linear, i.e., the condition in (12) simplifies to exceedances of $r(X)$ above $u = b_n$, a large n is equivalent to a large threshold $u \in \mathbb{R}$. In this case, the random variable $r(P)$ follows a generalized Pareto distribution with tail index $\xi \in \mathbb{R}$, scale $a_n > 0$ and location $b_n \in \mathbb{R}$.

Generalized r -Pareto processes offers a simple and flexible solution to model extremes of random fields. It is the main building block of the methodology proposed here to create, or enlarge, network of monitoring stations, for optimal monitoring of extreme events.

3.2 A flexible model for station networks

We now propose a model to find an optimal sequential sampling design in the sense of (1) when some a priori information of the physical process under consideration is available. For the Sihl river, as presented in Section 1, three monitoring stations are installed inside the basin and radar observations cover the whole region, providing information about the intensity and the structure of extreme rainfall in the region. The goal of such an analysis is to leverage all available data and propose guidelines as to where new stations should be installed for optimal monitoring of extremes.

More precisely, we suppose that, for a risk function r , the distribution of r -exceedances of the process X over the threshold $u \in \mathbb{R}$ can be approximated by a generalized r -Pareto process P as in (12). In this case, the process is allowed to have both non-stationary marginal tail distributions and potentially non-stationary extremal dependence. We also suppose that it is possible to estimate the parameters of P from the available data, i.e., that we have estimates of the functions \hat{a}_n , \hat{b}_n , $\hat{\xi}$ and of the dependence structure of W . In practice, this implies imposing a marginal parametric model such as

$$\left. \begin{aligned} a_n(s) &= f\{y(s)\} > 0, \\ b_n(s) &= g\{y(s)\} \in \mathbb{R}, \\ \xi(s) &= \xi \in \mathbb{R}, \end{aligned} \right\} s \in S,$$

where y refers to a vector of covariates, such as locations $s \in S$ or any field available throughout S like altitude or any spatially dense data set such as radar acquisitions. As mentioned in

Section 3.1, assuming constant ξ is common in environmental applications and is necessary to ensure that the risk can be defined on the original scale. We also suppose that the dependence of W is parametrized by a vector θ_W of parameters. For instance, if W is log-Gaussian, θ_W refers to the parameters of the semi-variogram function γ , which can be allowed to be non-stationary over space. Estimation procedures for a_n , b_n , ξ and θ_W can be found in [de Fondeville and Davison \(2021\)](#).

We also assume that the process X is observed at a set of locations $S_{\text{obs}} = \{s_1, \dots, s_{L_{\text{obs}}}\} \subset S$; the latter could be empty if no station measures are available and alternative sources of data can be leveraged. We denote by L_{samp} the number of new sites, i.e., the size of the network extension. This parameter is usually determined by practical constraints and available budget. With a non-stationary marginal behaviour, and potentially dependence, finding an optimal sampling design is not trivial, so, as in 2.4, we approximate numerically equation (1) with a finite number of potential candidate sites, i.e., we use a grid over S of size L_{grid} , whose size is determined by the resolution of the covariates y . With this setting, the number of sets of candidate sites grows exponentially with L_{samp} , getting quickly intractable for $L_{\text{samp}} > 2$. As detailed in Section 2.4, we propose a sequential procedure to solve (1); this provides a reasonable approximation of the solution while being computationally efficient. A sequential solution also reflects fields practices as in general new weather stations are installed sequentially, as this is a time consuming and costly process. The procedure is summarized by Algorithm 2 and combines an empirical estimator of the r -exceedance probabilities with simulations from the fitted generalized r -Pareto process. For the supremum functional, Algorithm 2 provides an exact solution to sequential designs as it was proved in Section 2.4. Note that, for instance, if the risk functional is linear and $u = r(b_n)$, then we can simply set $I = 1$, as by definition, all the elements of the simulation set P_n satisfies $r(P_n) \geq u$.

Algorithm 2: Algorithm for near-optimal sequential sampling design to monitor extremes

Input: S_{obs} , S_{grid} , u , a_n , b_n , ξ and θ_W ;
number of desired new sampling points L_{samp} , number of simulations N ;
Simulate N generalized r -Pareto processes P_n with parameters (ξ, θ_W) ;
Compute $I = N^{-1} \sum_{j=1}^N 1\{r_{S_{\text{grid}}}(a_n P_j + b_n) \geq u\}$;
Set $S_{\text{samp}} = \emptyset$;
for l from 1 to L_{samp} **do**
 for k in 1 to L_{grid} **do**
 Set $R[k] = |I - N^{-1} \sum_{j=1}^N 1\{r_{s_k \cup S_{\text{samp}} \cup S_{\text{obs}}}(a_n P_j + b_n) \geq u\}|$;
 end
 Set $S_{\text{samp}} = S_{\text{samp}} \cup s_{k_{\text{max}}}$ where $k_{\text{max}} = \arg \max_k R[k]$
end
return S_{samp} .

4 Optimal network for the Sihl river basin

To study rainfall in the region of Zurich, we can rely on the existing network of weather stations. The Sihl river basin itself contains only three monitoring stations. For improved model inference, we estimate the model using the measurements available in the coloured region in Figure 1, which includes up to 15 monitoring stations. For all these sites, MeteoSwiss provides hourly

mean rainfall with measurement from January 1st 2013 to March 2020 for half of them, while the 7 others have records starting between 2014 and 2016. Thus the times series have between 30000 and 62000 measures. One station outside the river basin has been installed in 2019 and therefore does not include enough measurements to be safely included.

To estimate a model for a generalized r -Pareto process, we can also leverage radar products. More precisely the CombiPrecip data set (Sideris et al., 2014; Gabella et al., 2017; Panziera et al., 2018) produced by MeteoSwiss provides estimates of hourly rainfall accumulation since 2013 on dense grid of 1km resolution. Earlier measurements are also available but inconsistent with recent acquisition due to hardware and processing changes in 2013. The Sihl river basin is orographically homogeneous and located at a reasonable distance from the radar, so the estimated rain fields can be assumed to be fairly homogeneous and free from processing biases. These measures, as the result of some processing, are however not reliable by themselves, i.e., their link with station measurement is unknown. We however suppose that the radar estimates present spatial variations similar to the true underlying rain field. Thus, we use radar measurements, first, as covariate to extrapolate the tail marginal model away from existing weather stations and, second, to estimate the model for extremal dependence.

4.1 Marginal model

In order to use Algorithm 2, we need first to estimate the functions a_n , b_n and the tail index $\xi \in \mathbb{R}$. To do so, we assume the following parametric model

$$\left. \begin{aligned} a_n(s) &= a \in (0, \infty), \\ b_n(s) &= b_1 + b_2 \times y(s), \\ \xi(s) &= \xi \in \mathbb{R}, \end{aligned} \right\} s \in S, \quad (13)$$

where y is a covariate derived from radar measurements. This model has been chosen following a preliminary analysis, where generalized Pareto distributions were fitted independently for each of the 14 stations and various thresholds: we found both the scale and tail index parameters to be homogeneous across S and ξ to be stable around quantiles 0.995 of the observational series; this represents between 150 and 300 exceedances per station, and about 2.5% to 5% of wet days. We explored several candidates for the covariate y , including local quantiles at different levels, and average rainfall accumulation, both for wet days only and overall series; we found the later to have about 95% correlation with empirical 0.995 quantiles from the station measurements. We thus chose the later as covariate in the parametric model (13); its spatial variation is displayed in Figure 1. Then using a least squares algorithm, we obtain $\hat{b}_1 = 1.14(0.34)$ and $\hat{b}_2 = 20.8(2.1)$; numbers in the brackets refer to estimated standard deviations. The corresponding model \hat{b}_n is displayed in Figure 4 and gives values higher than the corresponding empirical quantiles of the radar product. We then use independent likelihood to estimate the common scale $\hat{a} = 1.87(0.05)$ and tail index $\hat{\xi} = 0.33(0.02)$. The fit is assessed by visual inspection of the QQ-plots given in Appendix C, which is particularly convincing as it accommodate about 3200 exceedances from 14 stations with only 4 parameters. It is not surprising that such a simple model presents a good level of performance as the region under consideration is relatively small, approximately 2000km², with limited variations in altitude and is thus fairly homogeneous from an hydrological perspective.

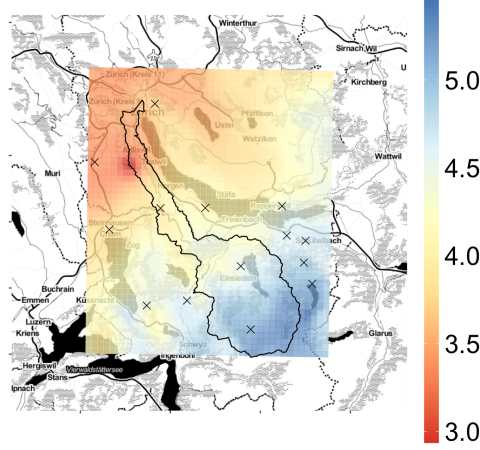


Figure 4: Estimated location model \hat{b}_n . The estimate is obtained using a least squares algorithm with radar based hourly mean rainfall as covariate. The solid black line delimits the Sihl river basin and black crosses represent the location of weather stations.

4.2 Dependence model

For generalized r -Pareto processes, extremal dependence is fully characterized by the angular component W , for which we propose to use a log-Gaussian process. More precisely,

$$W(s) = \frac{\exp\{G(s) - \sigma^2(s)/2\}}{\|\exp(G - \sigma^2/2)\|_1}, \quad (14)$$

where $\sigma^2(s)$ is the variance at location $s \in S$ of a zero mean Gaussian process G . We further assume that G has stationary increments, i.e., its semi-variogram function $\gamma(s, s') = \text{var}\{G(s') - G(s)\}$ is a function of the distance $h = s' - s$. We remind that in this case, the pairwise extremal dependence, as summarized by the extremogram, is linked through the closed form (11) to γ , for which we impose parametric model. We choose (Schlather and Moreva, 2017)

$$\gamma(h) = \frac{(1 + \|Ah/\lambda\|^\alpha)^{\beta/\alpha-1}}{2^{\beta/\alpha} - 1} \quad (15)$$

where $0 < \alpha < 2$ and $\beta < 2$ respectively drive the smoothness and long range behaviour of the process, $\lambda > 0$ is a scale parameter and A is a geometrical anisotropy matrix

$$A = \begin{bmatrix} \cos \delta & -\sin \delta \\ \kappa \sin \delta & \kappa \cos \delta \end{bmatrix},$$

with $\kappa > 0$ and $\delta \in (0, \pi/4)$. The model (15) is particularly attractive for modelling extremal dependence as, when $\beta < 0$, the semi-variogram function is bounded, while when $0 < \beta < 2$, $\gamma(h) \rightarrow \infty$ as $h \rightarrow \infty$, meaning that the process tends to be independent for increasingly large distances.

The extremogram can be estimated from the observations with

$$\hat{\rho}(h) = \frac{\sum_{i=1}^n 1\{X_i(s+h) \geq u_q(s+h), X_i(s) \geq u_q(s)\}}{1\{\sum_{i=1}^n X_i(s) \geq u_q(s)\}} \quad (16)$$

where $u_q(s)$ is the q^{th} quantile of X at location s , $q \in (0, 1)$ close enough to 1. We apply equation (16) on radar rainfall measurements with quantile level $q = 0.995$. We then fit a parametric model for the semi-variogram function γ using a least squares procedure.

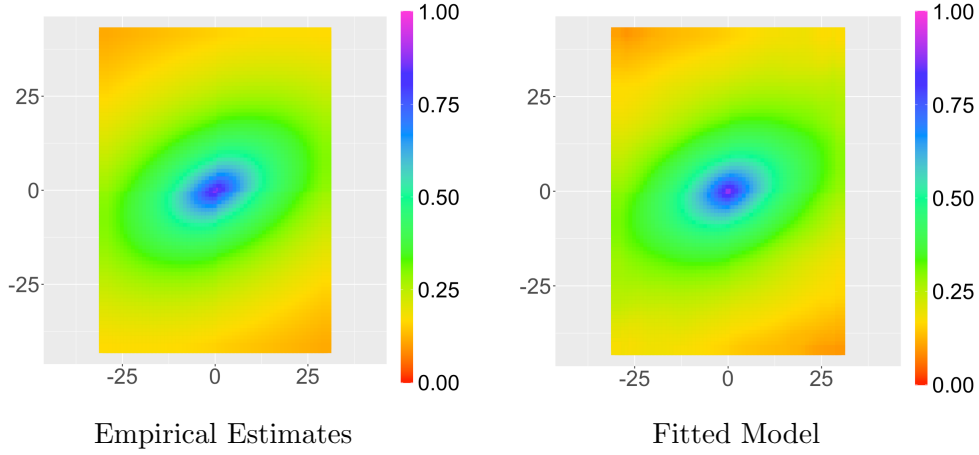


Figure 5: Empirical (left) and modelled (right) pairwise dependence estimated from radar rainfall measurements.

Figure 5 displays the empirical estimates against the estimated model. We observe a rather strong dependence up to 20km especially in the north-west direction, which drops quite quickly after 25km. These estimates are consistent with the observation that at such a fine scale, rainfall events tends to be localized in regions with diameters of no more than few dozens of kilometers.

4.3 New measurement stations in the Sihl Basin

Algorithm 2 relies on the generation of large samples of generalized r -Pareto processes, i.e., simulations of the angular component W , for which a detailed algorithm can be found in Appendix D. The model's output for the risk functional $r(X) = \sup_{s \in S} X(s)$ with threshold $u = 20\text{mm}$ and 10^5 simulations are displayed in Figure 6 for sequential extensions by 10 and 20 stations.

We also observe that as the number of sites increases, recommended locations tend to be located on the boundaries of the region, consistently with the results of Section 2.3. The very first station to be added is located in Zurich at the train station, however its relevance is limited as a station is already installed few kilometers away from the recommended location, as it can be seen in the Figure 1. The algorithm could be adapted to account for this phenomenon by extending the region by a few kilometers in all directions, mitigating the boundary effect but allowing for false positive when the network is used for early warning. The Sihl river basin also includes three stations that are manually operated by MeteoSwiss but can unfortunately not be leveraged for statistical analysis due to the temporal irregularity of the measurements. In Figure 6, we can see that Algorithm 2 suggests to automate one of them for the 20 stations scenario.

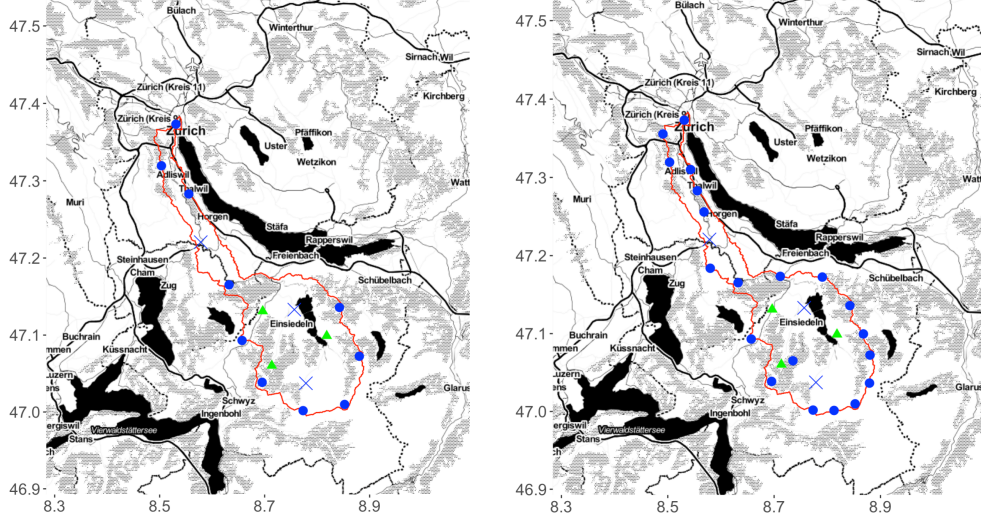


Figure 6: Locations of 10 (left) and 20 (right) new weather stations for optimal monitoring of extreme rainfall inside the Sihl river basin with sequential sampling designs. Blue crosses: Existing stations; blue dots: new stations; plain red line: basin limit; green triangles: existing manual measurements stations.

5 Discussion

In this work, we propose a new principle for sampling designs aiming to achieve optimal monitoring of extremes. We study the theoretical properties of the induced point patterns when monitoring the supremum of stationary stochastic processes whose dependence is assumed to decrease with distance. We obtain sampling designs resulting from a compromise between inter-location distance maximization and a boundary effect whose influence is determined by the strength of dependence. We also propose a tractable algorithm, relying on sequential designs, to approximate our criterion for optimal sampling. When data is available in the region of interest, as it is the case of Sihl river basin, we propose a model, based on generalized r -Pareto processes, allowing us to propose recommendations for possibly extending the existing network by 10 and 20 stations.

Compared to other approaches, such as Gaussian processes, the proposed methodology allows a principled modelization of the tail of distribution, by using an asymptotically justified framework. The dependence structure that can be modelled is quite flexible, and could be made non-stationary using techniques such as [Fuglstad et al. \(2015\)](#) or [Fouedjio et al. \(2015\)](#), when a sufficiently large number of stations is already in operation. Our procedure can be efficiently implemented using the algorithm described in the Section 2.4. This contribution should also prove to be useful in a wide variety of settings. For instance, [Chang et al. \(2007\)](#), due to the absence of better and more specialized alternatives, resorted to use a multivariate Gaussian-Inverse Wishart hierarchical Bayesian distribution to monitor air pollution. However, as they say, “the primary role – of air pollution monitoring networks – is the detection of noncompliance with air quality standards based on extremes designed to protect human health”, and thus our model, which is tailored for extremes monitoring, would be particularly relevant in this context.

Finally, the proposed model for the Sihl river relies on generalized r -Pareto processes, for which the strength of extremal dependence is ‘frozen’ above a given level of intensity: the model is thus conservative by nature and extremal dependence might be over-estimated above

the quantile of reference. Asymptotic models cannot accommodate for decreasing trends of dependence with intensity that is observed in multiple environmental applications and sub-asymptotic alternatives for functional peaks-over-threshold should then be considered. However, only very few of them exists (Davison and Gholamrezaee, 2012; Huser et al., 2017; Huser and Wadsworth, 2019) and would either not be tractable or sufficiently realistic in the application considered in this work.

References

- Adler, R. J. and Taylor, J. E. (2007). *Random Fields and Geometry*. Springer, New-York.
- Arnaud, A., Bect, J., Couplet, M., Pasanisi, A., and Vazquez, E. (2010). Évaluation d'un Risque d'Inondation Fluviale par Planification Séquentielle d'Expériences. In *compte-rendus des 42èmes Journées de Statistique*.
- Azzimonti, D., Bect, J., Chevalier, C., and Ginsbourger, D. (2016). Quantifying Uncertainties on Excursion Sets Under a Gaussian Random Field Prior. *SIAM-ASA Journal on Uncertainty Quantification*, 4(1):850–874.
- Azzimonti, D., Ginsbourger, D., Chevalier, C., Bect, J., and Richet, Y. (2019a). Adaptive Design of Experiments for Conservative Estimation of Excursion Sets. *Technometrics*, 63(1):13–26.
- Azzimonti, D., Ginsbourger, D., Rohmer, J., and Idier, D. (2019b). Profile Extrema for Visualizing and Quantifying Uncertainties on Excursion Regions: Application to Coastal Flooding. *Technometrics*, 61(4):474–493.
- Balkema, A. A. and de Haan, L. (1974). Residual Life Time at Great Age. *The Annals of Applied Statistics*, 2(5):792–804.
- Bect, J., Ginsbourger, D., Li, L., Picheny, V., and Vazquez, E. (2012). Sequential Design of Computer Experiments for the Estimation of a Probability of Failure. *Statistics and Computing*, 22(3):773–793.
- Bezzola, G. R. and Hegg, C. (2007). Ereignisanalyse Hochwasser 2005, Teil 1 - Prozesse, Schäden und erste Einordnung. Technical report, Bundesamt für Umwelt und Eidgenössische Forschungsanstalt für Wald, Schnee und Landschaft (WSL).
- Chang, H., Fu, A. Q., Le, N. D., and Zidek, J. V. (2007). Designing Environmental Monitoring Networks to Measure Extremes. *Environmental and Ecological Statistics*, 14(3):301–321.
- Chevalier, C., Ginsbourger, D., Picheny, V., Bect, J., Vazquez, E., and Richet, Y. (2014). Fast Parallel Kriging-Based Stepwise Uncertainty Reduction With Application to the Identification of an Excursion Set. *Technometrics*, 56(4):455–465.
- Cloke, H. L. and Pappenberger, F. (2009). Ensemble Flood Forecasting: a Review. *Journal of Hydrology*, 375(3-4):613–626.
- Davis, R. A. and Mikosch, T. (2009). The Extremogram: a Correlogram for Extreme Events. *Bernoulli*, 15(4):977–1009.
- Davison, A. C. (1984). Modelling Excesses over High Thresholds, with an Application. In de Oliveira, J. T., editor, *Statistical Extremes and Applications*, pages 461–482. Reidel, Dordrecht.

- Davison, A. C. and Gholamrezaee, M. M. (2012). Geostatistics of Extremes. *Proceedings of the Royal Society A: Mathematical, Physical and Engineering Sciences*, 468(2138):581–608.
- de Fondeville, R. and Davison, A. C. (2018). High-dimensional Peaks-over-threshold Inference. *Biometrika*, 105(3):575–592.
- de Fondeville, R. and Davison, A. C. (2021). Functional Peaks-over-threshold Analysis. *arXiv:2002.02711*.
- Dombry, C. and Ribatet, M. (2015). Functional Regular Variations, Pareto Processes and Peaks Over Thresholds. *Statistics and Its Interface*, 8(1):9–17.
- Engelke, S., de Fondeville, R., and Oesting, M. (2019). Extremal Behaviour of Aggregated Data with an Application to Downscaling. *Biometrika*, 106(1):127–144.
- Ferreira, A., de Haan, L., and Zhou, C. (2012). Exceedance Probability of the Integral of a Stochastic Process. *Journal of Multivariate Analysis*, 105(1):241–257.
- Fisher, R. A. and Tippett, L. H. C. (1928). Limiting Forms of the Frequency Fistribution of the Largest or Smallest Member of a Sample. *Mathematical Proceedings of the Cambridge Philosophical Society*, 24(2):180–190.
- Fouedjio, F., Desassis, N., and Romary, T. (2015). Estimation of space deformation model for non-stationary random functions. *Spatial Statistics*, 13:45–61.
- Fuglstad, G.-A., Lindgren, F., Simpson, D., and Rue, H. (2015). Exploring a New Class of Non-stationary Spatial Gaussian Random Fields with Varying Local Anisotropy. *Statistica Sinica*, 25(1):115–133.
- Furrer, E. M. and Katz, R. W. (2008). Improving the Simulation of Extreme Precipitation Events by Stochastic Weather Generators. *Water Resources Research*, 44(12):1–13.
- Gabella, M., Speirs, P., Hamann, U., Germann, U., and Berne, A. (2017). Measurement of Precipitation in the Alps Using Dual-polarization C-Band Ground-based Radars, the GPMSpace-borne Ku-Band Radar, and Rain Gauges. *Remote Sensing*, 9(11):1147–1166.
- Gnedenko, B. (1943). Sur la Distribution Limite du Terme Maximum d’une Série Aléatoire. *Annals of Mathematics*, 44(3):423–453.
- Hainy, M., Müller, W. G., and Wagner, H. (2016). Likelihood-free Simulation-based Optimal Design with an Application to spatial extremes. *Stochastic Environmental Research and Risk Assessment*, 30(2):481–492.
- Huser, R., Opitz, T., and Thibaud, E. (2017). Bridging Asymptotic Independence and Dependence in Spatial Extremes Using Gaussian Scale Mixtures. *Spatial Statistics*, 21(1):166–186.
- Huser, R. and Wadsworth, J. L. (2019). Modeling Spatial Processes with Unknown Extremal Dependence Class. *Journal of the American Statistical Association*, 114(525):434–444.
- Jones, D. R., Schonlau, M., and Welch, W. J. (1998). Efficient Global Optimization of Expensive Black-Box Functions. *Journal of Global Optimisation*, 13(4):455–492.
- Ledford, A. W. and Tawn, J. A. (1996). Statistics for Near Independence in Multivariate Extreme Values. *Biometrika*, 83(1):169–187.

- Li, J. and Zimmerman, D. L. (2015). Model-based Sampling Design for Multivariate Geostatistics. *Technometrics*, 57(1):75–86.
- Müller, W. G. and Zimmerman, D. L. (1999). Optimal Designs for Variogram Estimation. *Environmetrics*, 10(1):23–37.
- Panziera, L., Gabella, M., Germann, U., and Martius, O. (2018). A 12-year Radar-based Climatology of Daily and Sub-daily Extreme Precipitation over the Swiss Alps. *International Journal of Climatology*, 38(10):3749–3769.
- Pickands, J. (1975). Statistical Inference using Extreme Order Statistics. *The Annals of Statistics*, 3(1):119–131.
- Pronzato, L. and Müller, W. G. (2012). Design of Computer Experiments : Space Filling and Beyond. *Statistics and Computing*, 22(1):681–701.
- Pukelsheim, F. (2006). *Optimal Design of Experiments*. Society for Industrial and Applied Mathematics (SIAM), Philadelphia.
- Rootzén, H., Segers, J., and Wadsworth, J. L. (2018a). Multivariate Generalized Pareto Distributions: Parametrizations, Representations, and Properties. *Journal of Multivariate Analysis*, 165(1):117–131.
- Rootzén, H., Segers, J., and Wadsworth, J. L. (2018b). Multivariate Peaks-over-thresholds Models. *Extremes*, 21(1):115–145.
- Rootzén, H. and Tajvidi, N. (2006). Multivariate Generalized Pareto Distributions. *Bernoulli*, 12(5):917–930.
- Santner, T. J., Williams, B. J., and Notz, W. I. (2018). *The Design and Analysis of Computer Experiments*. Springer, New York, second edition.
- Schlather, M. and Moreva, O. (2017). A Parametric Model Bridging Between Bounded and Unbounded Variograms. *Stat*, 6(1):47–52.
- Sideris, I. V., Gabella, M., Erdin, R., and Germann, U. (2014). Real-time Radar-rain-gauge Merging Using Spatio-temporal Co-kriging with External Drift in the Alpine Terrain of Switzerland. *Quarterly Journal of the Royal Meteorological Society*, 140(680):1097–1111.
- Tillé, Y. and Wilhelm, M. (2017). Probability Sampling Designs: Principles for Choice of Design and Balancing. *Statistical Science*, 32(2):176–189.
- Tobler, W. . R. . (1970). A Computer Movie Simulating Urban Growth in the Detroit. *Economic Geography*, 46(suppl):234–240.
- Wang, Y. and Stoev, S. A. (2013). Conditional Sampling for Spectrally Discrete Max-stable Random Field. *Advances in Applied Probability*, 43(2):461–483.
- Zhang, T. (2011). Adaptive Forward-backward Greedy Algorithm for Learning Sparse Representations. *IEEE Transactions on Information Theory*, 57(7):4689–4708.
- Zidek, J. V. and Zimmerman, D. L. (2019). Monitoring Network Design. In Gelfand, A., Fuentes, M., Hoeting, J. A., and Smith, R. L., editors, *Handbook of Environmental and Ecological Statistics*, pages 499 – 522. CRC Press, Boca Raton.

A Simulation parameters for Figure 2

In Figure 2, estimates are obtained by estimating of empirical probabilities using 1000 samples of each processes. The procedure is repeated 1000 times to also obtain 95% confidence intervals. Both Gaussian and generalized r -Pareto processes are defined on $S = [-6; 6]$ and simulated over a regular grid with lag 0.1. For the Gaussian processes, we use semi-variogram function

$$\gamma_G(h) = \sigma[1 - \exp\{(h/\lambda)^\alpha\}], \quad h > 0,$$

with $\sigma = 2$, $\alpha = 1.5$, $\lambda = 100$ for the strong dependence case and $\lambda = 1$ for the weakly dependent case. Generalized r -Pareto processes are constructed using model (14), for which we use:

- for the strong dependence case,

$$\gamma_W(h) = \sigma[1 - \exp\{(h/\lambda)^\alpha\}], \quad h > 0,$$

with $\sigma = 2$, $\alpha = 1.5$, and $\lambda = 10$;

- for the weak dependence case,

$$\gamma_W(h) = (h/\lambda)^\alpha, \quad h > 0$$

with $\alpha = 1.5$, and $\lambda = 2.5$.

B Proof of Theorem 1

Suppose that X is a stationary process on $C(\mathbb{R}^d)$ with $d > 0$. For simplicity, we prove Theorem 1 for $d = 1$ but generalization to $d > 1$ can be done using similar arguments. We study the compact subset $[0, S]$ with $S > 0$ and let $\tilde{s} \in [0, S]$ and consider a threshold $u \in \mathbb{R}$ such that $\Pr\{X(s) \geq u\} > 0$. Let $h \in H =]0, S - \tilde{s}]$ and define the function $\mu : H \rightarrow \mathbb{R}$ such that

$$\begin{aligned} \mu(h) &= \Pr\left\{ \sup_{s \in [h, \tilde{s}+h]} X(s) \geq u, \quad \sup_{s \in [0, S] \setminus [h, \tilde{s}+h]} X(s) < u \right\} \\ &= \Pr\left\{ \sup_{s \in [h, \tilde{s}+h]} X(s) \geq u \right\} - \Pr\left\{ \sup_{s \in [h, \tilde{s}+h]} X(s) \geq u, \quad \sup_{s \in [0, S] \setminus [h, \tilde{s}+h]} X(s) \geq u \right\} \end{aligned}$$

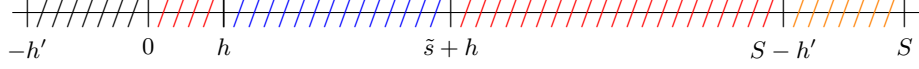
and we aim to prove that $\mu(h)$ is decreasing if $h < (S - \tilde{s})/2$ and increasing when $h > (S - \tilde{s})/2$, i.e., $\mu(h)$ is a decreasing function of the distance to the boundaries of $d([h, h + \tilde{s}], \partial S) = \inf_{s \in [h, h + \tilde{s}]} \inf_{s' \in \partial S} d(s, s')$.

For any $h' \in [0, \frac{S - (\tilde{s} + h)}{2}]$, using the stationarity of X , we have

$$\begin{aligned} \mu(h + h') &= \Pr\left\{ \sup_{s \in [h+h', \tilde{s}+h+h']} X(s) \geq u, \quad \sup_{s \in [0, S] \setminus [h+h', \tilde{s}+h+h']} X(s) < u \right\}, \\ &= \Pr\left\{ \sup_{s \in [h, \tilde{s}+h]} X(s) \geq u, \quad \sup_{s \in [-h', S-h'] \setminus [h, \tilde{s}+h]} X(s) \leq u \right\}, \\ &= \Pr\left\{ \sup_{s \in [h, \tilde{s}+h]} X(s) \geq u, \quad \sup_{s \in [-h', 0] \setminus [h, \tilde{s}+h]} X(s) \leq u, \quad \sup_{s \in [0, S-h'] \setminus [h, \tilde{s}+h]} X(s) \leq u \right\}, \\ &= \Pr\{A(h, h'), \sup_{s \in [-h', 0] \setminus [h, \tilde{s}+h]} X(s) \leq u\}, \\ &= \Pr\{A(h, h')\} - \Pr\{A(h, h'), \sup_{s \in [-h', 0]} X(s) \geq u\} \end{aligned}$$

where $A(h, h') = \{\sup_{s \in [h, \tilde{s}+h]} X(s) \geq u, \sup_{[0, S-h'] \setminus [h, \tilde{s}+h]} X(s) \leq u\}$. Similarly, we have

$$\mu(h) = \Pr\{A(h, h')\} - \Pr\{A(h, h'), \sup_{s \in [S-h', S]} X(s) \geq u\}.$$



The difference $\mu(h + h') - \mu(h)$ is thus

$$\begin{aligned} \mu(h + h') - \mu(h) &= \Pr\left\{\sup_{[0, S-h'] \setminus [h, \tilde{s}+h]} X(s) \leq u, \sup_{s \in [h, \tilde{s}+h]} X(s) \geq u, \sup_{s \in [S-h', S]} X(s) \geq u\right\} \\ &\quad - \Pr\left\{\sup_{[0, S-h'] \setminus [h, \tilde{s}+h]} X(s) \leq u, \sup_{s \in [h, \tilde{s}+h]} X(s) \geq u, \sup_{s \in [-h', 0]} X(s) \geq u\right\} \end{aligned}$$

The condition $\sup_{[0, S-h'] \setminus [h, \tilde{s}+h]} X(s) \leq u$ defines a hitting scenario H_1 for which X exceeds u exclusively on $[h, \tilde{s} + h]$ and $[-h', 0]$. Following Assumption 1, we have

$$\Pr\left\{\sup_{s \in [h, \tilde{s}+h]} X(s) \geq u, \sup_{s \in [S-h', S]} X(s) \geq u, H_1\right\} \geq \Pr\left\{\sup_{s \in [h, \tilde{s}+h]} X(s) \geq u, \sup_{s \in [-h', 0]} X(s) \geq u, H_1\right\} \quad (17)$$

if

$$\text{dist}([h, \tilde{s} + h], [-h', 0]) = h > \text{dist}([h, \tilde{s} + h], [S - h', S]) = S - h' - (\tilde{s} + h),$$

or equivalently if $h > (S - h' - \tilde{s})/2$. Inequality (17) is reversed when $h < (S - h' - \tilde{s})/2$, which concludes the proof of Theorem 1.

C Qq-plots for the station tail distributions

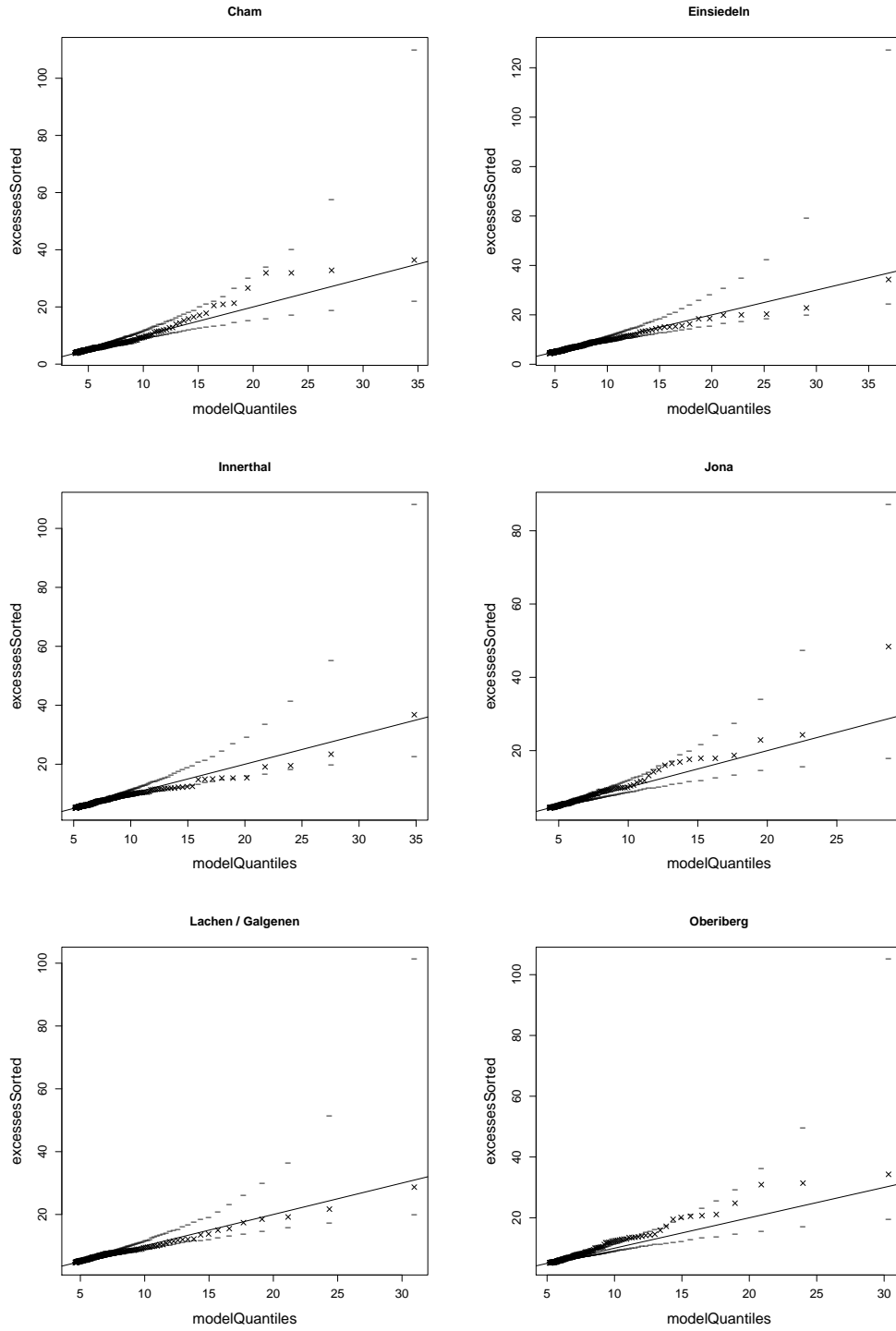


Figure 7: QQ-plot of the fitted model for the tail distribution of the 6 first, out of 14, stations used in the analysis with 95% confidence intervals obtained by parametric bootstrap.

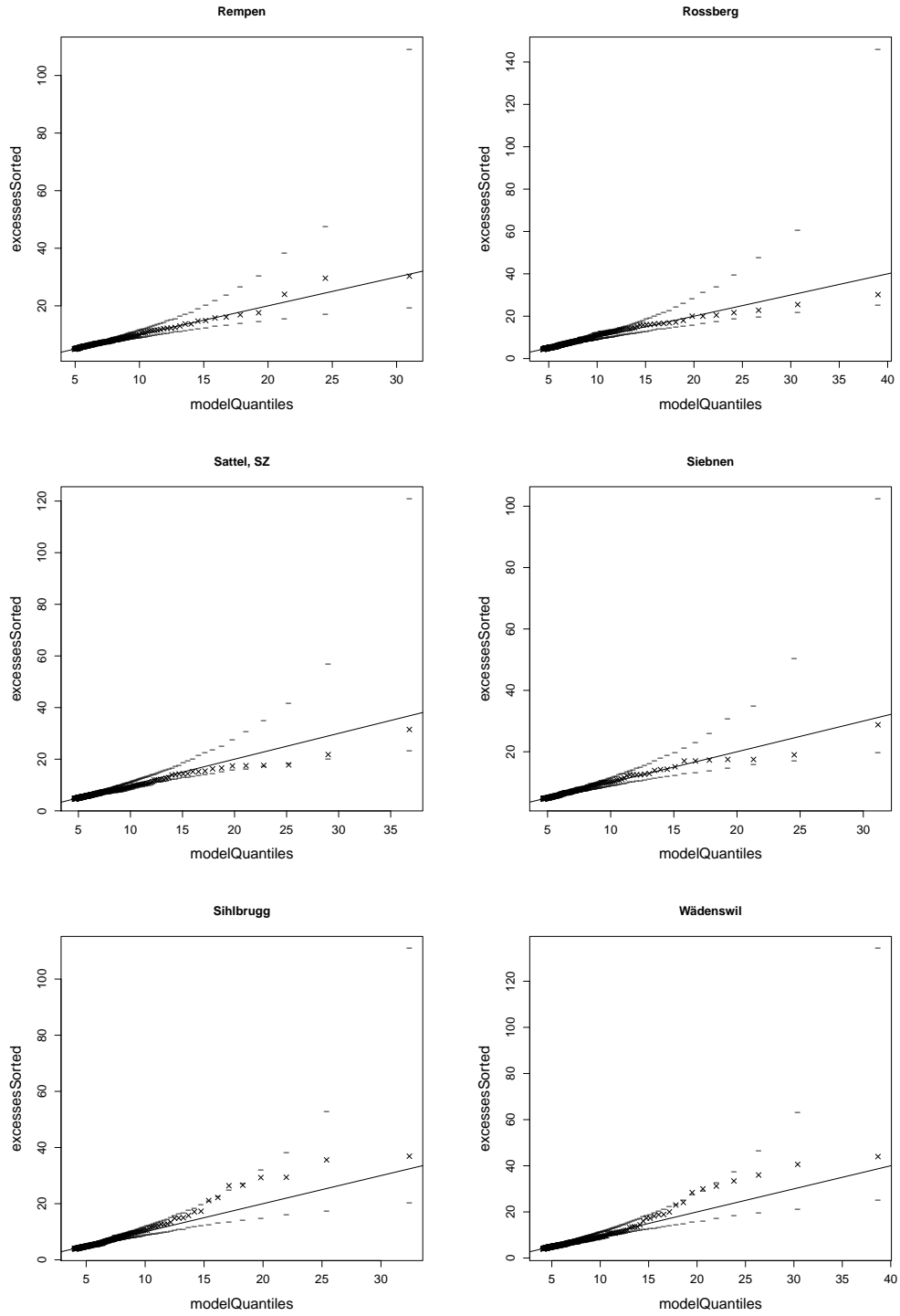


Figure 8: QQ-plot of the fitted model for the tail distribution of stations 7 to 12 used in the analysis with 95% confidence intervals obtained by parametric bootstrap.

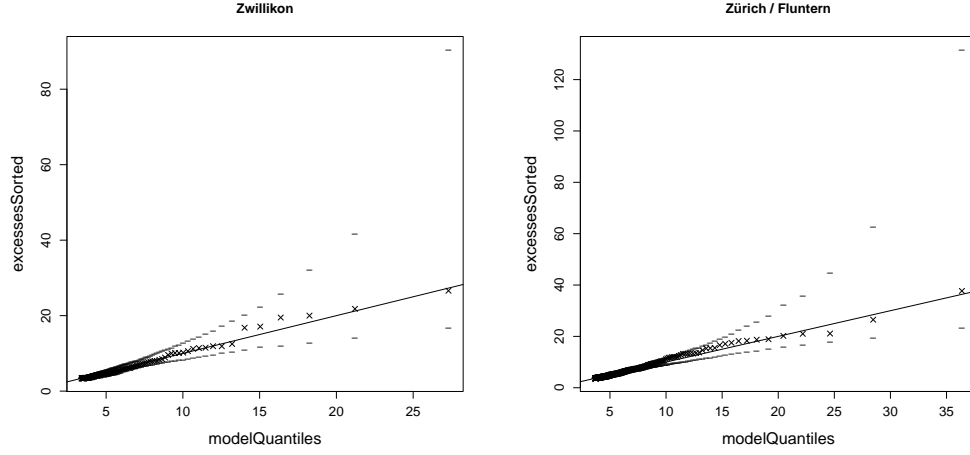


Figure 9: QQ-plot of the fitted model for the tail distribution of the last 2 stations used in the analysis with 95% confidence intervals obtained by parametric bootstrap.

D Simulation algorithm log-Gaussian generalized r -Pareto processes

In the following, we use the convention that, for an array M , $M[i,]$ and $M[, i]$ denote respectively the i -th line and column respectively.

Algorithm 3: Simulation of N realizations of log-Gaussian angular measure (de Fondeville and Davison, 2021).

Input semi-variogram γ , grid coordinates S_{grid} , risk functional r , and threshold u ;
Input number of simulations N ;
Optional: input parameters a , b and ξ ;
Compute semi-variogram matrix $\Gamma = \gamma(s_{1:L_{\text{grid}}}, s_{1:L_{\text{grid}}})$;
Compute conditional covariance matrix $\Sigma_{ij} = \Gamma_{i1} + \Gamma_{j1} - \Gamma_{ij}$;
Initialise Sims, a matrix of size $N \times L_{\text{grid}}$ with all entries equal to 0;
Simulate N Gaussian processes with zero mean and covariance Σ and set
 $\text{Sims}[:, -1] = \text{Gaussian}(0, \Sigma)$;
for n from 1 to N **do**
 Generate unit Pareto variable R ;
 Set $\text{Sims}[n, :] = R \cdot \frac{\exp(\text{Sims}[n, :])}{\|\exp(\text{Sims}[n, :])\|_1}$;
 while $r \left\{ (\text{Sims})[n, :]^\xi - 1 \right\} \frac{a}{\xi} + b < u$ **do**
 Generate a new sample from $G' = \text{Gaussian}(0, \Sigma)$;
 Generate unit Pareto variable R' ;
 Set $\text{Sims}[n, :] = R' \cdot \frac{\exp(c(0, G'))}{\|\exp(c(0, G'))\|_1}$
 end
 Set $\text{Sims}[n, :] = ((\text{Sims})[n, :]^\xi - 1) \frac{a}{\xi} + b$;
end
return S_{samp} .
